A density functional perturbative approach for simple fluids: the structure of a nonuniform

Lennard-Jones fluid at interfaces

A density functional perturbative approach for simple fluids: the structure of a nonuniform Lennard-Jones fluid at interfaces

Soon-Chul Kim[1] **and Song Hi Lee**[2]

[1] Department of Physics, Andong National University, Andong 760-749, Korea
[2] Department of Chemistry, Kyungsung University, Pusan 608-736, Korea

E-mail: sckim@andong.ac.kr

Abstract
A density functional perturbation approximation (DFPT), which is based both
on the fundamental-measure theory (FMT) to the hard-sphere repulsion and
on the weighted-density approximations (WDAs) to the attractive contribution,
has been proposed for studying the structural properties of model fluids with
an attractive part of the potential. The advantage of the present theory is
the simplicity of the calculation of the weight function due to the attractive
contribution. It has been applied to predict the equilibrium particle density
distributions and adsorption isotherms of Lennard-Jones fluids at interfaces.
The theoretical results show that the present theory describes quite well the
adsorption isotherms of a Lennard-Jones ethane in a graphite slit pore as well
as the equilibrium particle density distributions of a Lennard-Jones fluid near
a planar slit pore.

1. Introduction

During the last few decades, considerable progress has been made in the understanding of
phenomena originating from the interaction of fluids with surfaces [1–3]. Various theoretical
approaches such as the density functional theories (DFTs) and the integral equation theories
(IETs) have been proposed for predicting the structural properties of model fluids at interfaces.
For the structural properties of model systems with an attractive part of the potential, the
density functional perturbation theories (DFPTs) are often used rather than the DFTs because
of their accuracy in actual applications. Many DFPTs are based on the so-called mean-field
approximation to the attractive term of the free energy, which is not accurate as is seen by
comparison with computer simulations, whereas our DFPTs (or second-order perturbation
theories) [4–6] are based on the macroscopic compressibility approximation (MCA) of Barker

and Henderson [7]; they require significant computational time when they are applied, but yield better results than the DFPTs based on the mean-field approximation.

On the other hand, it is generally known that the weighted-density approximations (WDAs) based on the 'coarse-grained' densities explain the structural and thermodynamic properties of the hard-sphere systems very well [1, 2]. However, many applications of the WDA methods are mainly restricted to hard-sphere repulsion. WDA methods for addressing an attractive contribution have been proposed by a few authors [8–11]. In the WDAs to the attractive contribution, the key point is how one chooses the weight density and weight function. It has been demonstrated that:

 (i) the WDA methods basically developed for the hard-sphere systems can be applied for studying the structure of model systems with an attractive part of the potential; and that
 (ii) the WDA methods applied to the attractive contribution can offer a significant increase in accuracy over the mean-field approximations for different kinds of simple fluids such as the sticky hard-sphere fluids [9] and the Lennard-Jones fluids [10, 11].

More recently, Patra and Ghosh [12] have proposed a simple WDA for studying the structure of a freely rotating fused-hard-sphere chain, where the higher-order WDA of Denton and Ashcroft [13] was employed to calculate the weight function. They had shown that it describes the structural properties of a hard-sphere polyatomic fluid with the chain connectivity very well. Here, the main benefit is the simplicity of calculation of the weight function. The success of various WDA methods in addressing the attractive contribution encourages one to apply WDA methods for studying the structure of a Lennard-Jones fluid.

The present paper is organized as follows. In section 2, we will propose a DFPT which is based on the fundamental-measure theory (FMT) [14] for the hard-sphere repulsion and the WDAs to the attractive contribution. In section 3, we apply it to study the structure of Lennard-Jones fluids in planar slit pores. We compare our results with computer simulations and the DFPTs based on the first-order and second-order perturbation theories for a liquid. Finally, a brief discussion on the strengths and weaknesses of the present approximation is included.

2. Density functional perturbation theory (DFPT)

In the DFPT, the equilibrium particle density distribution $\rho(\vec{r})$ is described via the minimum of the grand canonical potential $\Omega[\rho]$ satisfying the Euler–Lagrange relation $\delta\beta\Omega[\rho]/\delta\rho(\vec{r}) = 0$ [1, 2]. If the inhomogeneous fluid is in contact with the homogeneous bulk fluid, its chemical potential μ is equal to that of the homogeneous bulk fluid. Then, the density profile equation is given, after some manipulations, as

$$\ln\left[\frac{\rho(\vec{r})}{\rho}\right] = -\beta u_{\text{ext}}(\vec{r}) + c_{\text{hs}}^{(1)}(\vec{r}; [\rho]) + c_{\text{att}}^{(1)}(\vec{r}; [\rho]) - c_{\text{hs}}^{(1)}(\rho) - c_{\text{att}}^{(1)}(\rho), \quad (1)$$

where ρ denotes the homogeneous bulk density, $\beta = 1/k_{\text{B}}T$ is the inverse temperature, k_{B} is Boltzmann's constant, and $\beta u_{\text{ext}}(r)$ is the external potential corresponding to the liquid–solid interaction. In equation (1), $c_{\text{hs}}^{(1)}(\vec{r}; [\rho])$ and $c_{\text{att}}^{(1)}(\vec{r}; [\rho])$ are the one-particle direct correlation functions (DCFs) corresponding to the inhomogeneous fluid, which are defined as

$$c_{\text{hs}}^{(1)}(\vec{r}; [\rho]) = -\frac{\delta\beta F_{\text{hs}}[\rho]}{\delta\rho(\vec{r})}, \qquad \text{and} \qquad c_{\text{att}}^{(1)}(\vec{r}; [\rho]) = -\frac{\delta\beta F_{\text{att}}[\rho]}{\delta\rho(\vec{r})}, \quad (2)$$

where $F_{\text{hs}}[\rho]$ is the free energy corresponding to the hard-sphere repulsion and $F_{\text{att}}[\rho]$ is the free energy corresponding to the attractive contribution.

For the Lennard-Jones fluids, the hard-sphere contribution is usually approximated by that of an equivalent hard-sphere fluid with the diameter d [7]. To approximate the free energy $F_{hs}[\rho]$ corresponding to the hard-sphere contribution, we use the FMT which is the most successful approximation for a hard-sphere system and was proposed by Rosenfeld and co-workers [14]. In this case, the one-particle DCF $c_{hs}^{(1)}(\vec{r}; [\rho])$ is simply given by

$$c_{hs}^{(1)}(\vec{r}; [\rho]) = -\int d\vec{s} \sum_{\alpha} \frac{\partial f[n_{\gamma}(\vec{s})]}{\partial n_{\alpha}(\vec{r})} \omega_{\alpha}(|\vec{r} - \vec{s}|), \tag{3}$$

where $f[n_{\alpha}(\vec{r})]$ is the excess free energy of a hard-sphere system per volume, $\omega_{\alpha}(r)$ is the weight function, and $n_{\alpha}(\vec{r}) = \int d\vec{s}\, \rho(\vec{s})\omega_{\alpha}(|\vec{r} - \vec{s}|)$ is the system-averaged fundamental geometric measure of the particles. Here, we do not describe the functional, $c_{hs}^{(1)}(\vec{r}; [\rho])$, in detail since it has been well documented elsewhere [14].

On the other hand, little is known about the excess free energy $F_{att}[\rho]$ of the attractive contribution. For this purpose, we introduce the hybrid weighted-density approximation (HWDA) which was introduced by Leidl and Wagner [15]. In this case, the excess free energy $F_{att}[\rho]$, which is a functional of the local density distribution, is given by

$$F_{att}[\rho] = \int d\vec{r}\, \rho(\vec{r}) f_{att}[\bar{\rho}(\vec{r})], \tag{4}$$

where $f_{att}(\rho)$ is the excess free energy per particle and the weight density $\bar{\rho}(\vec{r})$ is assumed as

$$\bar{\rho}(\vec{r}_1) = \int d\vec{r}_2\, \rho(\vec{r}_2)\omega_{att}(\vec{r}_1 - \vec{r}_2; \hat{\rho}) \tag{5}$$

with $\hat{\rho}[\rho] = 1/N \int d\vec{r}_1\, \rho(\vec{r}_1) \int d\vec{r}_2\, \rho(\vec{r}_2)\omega_{att}(\vec{r}_1 - \vec{r}_2; \hat{\rho})$. Then, the one-particle DCF $c_{att}^{(1)}(\vec{r}; [\rho])$ that appeared in equation (1) becomes, from equations (4) and (5),

$$c_{att}^{(1)}(\vec{r}_1; [\rho]) = \beta f_{att}[\bar{\rho}(\vec{r}_1)] + \int d\vec{r}_2\, \rho(\vec{r}_2)\beta f_{att}'[\bar{\rho}(\vec{r}_2)]\frac{\delta\bar{\rho}(\vec{r}_2)}{\delta\rho(\vec{r}_1)}, \tag{6}$$

where the prime denotes the derivative with respect to the density.

To determine the weight function $\omega_{att}(r, \rho)$, we use the higher-order WDA of Denton and Ashcroft [13] which was employed successfully for different types of complex fluid and recently examined by Patra and Ghosh [12] for the freely rotating fused-hard-sphere chain. In this case, the weight function is simply given by

$$\omega_{att}(r, \rho) = \frac{c_{att}^{(2)}(r, \rho)}{\int d\vec{r}\, c_{att}^{(2)}(r, \rho)}, \tag{7}$$

where $c_{att}^{(2)}(r, \rho)$ is the two-particle DCF corresponding to the attractive contribution and $w_{att}(r, \rho)$ satisfies the normalization condition $\int d\vec{r}\, w_{att}(r, \rho) = 1$. In the uniform limit, equation (6) satisfies

$$c_{att}^{(1)}(\rho) = \beta f_{att}(\rho) + \rho\beta f_{att}'(\rho) \tag{8}$$

since $\hat{\rho}[\rho] = \bar{\rho}(\vec{r}) = \rho$ and $\int d\vec{r}\, w_{att}(r, \rho) = 1$. Combined, equations (1), (3)–(8) constitute the density profile equation for the DFPT based on the HWDA and the higher-order WDA. As a comment, we note that in the original HWDA proposed by Leidl and Wagner [15], the weight function $\omega_{att}(r, \rho)$ is specified by the definition of the two-particle DCF $c_{att}^{(2)}(\vec{r}_1 - \vec{r}_2, \rho) \equiv -\delta^2\beta F_{att}[\rho]/\delta\rho(\vec{r}_1)\delta\rho_2(\vec{r}_2)|_{\rho(\vec{r})->\rho}$. In Fourier space, the weight function has a simple algebraic form such as

$$\rho f_{att}''(\rho)\omega_{att}(k, \rho)\omega_{att}(k, \rho) + 2f_{att}'(\rho)\omega_{att}(k, \rho) + \beta^{-1}c_{att}^{(2)}(k, \rho) = 0. \tag{9}$$

Equation (9) requires that $f_{att}(\rho)$ is consistent with the two-particle DCF $c_{att}^{(2)}(r, \rho)$, to satisfy the normalization condition $\int d\vec{r}\, w_{att}(r, \rho) = 1$.

3. Results and discussion

3.1. A Lennard-Jones fluid at a hard wall

As an application, a structureless hard wall is considered:

$$u_{ext}(z) = \begin{cases} \infty, & z < 0, \\ 0, & z > 0. \end{cases} \tag{10}$$

For a slit-like pore, the equilibrium particle density distribution just depends on z by a symmetry property, and not on x, y; $\rho(\vec{r}) = \rho(z)$ and $\hat{\rho}[\rho] = \rho$. Thus, we define the z-axis to be perpendicular to the walls. The density profile equation, equation (1), becomes

$$\ln\left[\frac{\rho(z)}{\rho}\right] = c_{hs}^{(1)}(z; [\rho]) + c_{att}^{(1)}(z; [\rho]) - c_{hs}^{(1)}(\rho) - c_{att}^{(1)}(\rho), \qquad \text{for } z > 0, \tag{11}$$

with the plane-averaged form $c^{(1)}(z; [\rho]) = \int_{-\infty}^{+\infty} dx \int_{-\infty}^{+\infty} dy\, c^{(1)}(\sqrt{x^2 + y^2 + z^2}; [\rho])$. To compare with the computer simulation, the Lennard-Jones potential $\phi_{LJ}(r)$ was cut off at r_c and shifted:

$$\phi_{CS}(r) = \begin{cases} \phi_{LJ}(r) - \phi_{LJ}(r_c) & \text{if } r < r_c, \\ 0 & \text{if } r > r_c, \end{cases} \tag{12}$$

where $\phi_{CS}(r)$ is the cut and shifted Lennard-Jones potential.

The FMT [14] proposed by Rosenfeld and co-workers was employed to calculate the one-particle DCF $c_{hs}^{(1)}(\vec{r}; [\rho])$ due to the hard-sphere repulsion. The effective hard-sphere diameter, d, was chosen according to the Barker–Henderson (BH) prescription [7]

$$d = \int dr\, [1 - \exp[-\beta\phi_{rep}(r)]], \tag{13}$$

where $\beta\phi_{rep}(r)$ is the repulsive part of a cut and shifted Lennard-Jones potential $\phi_{CS}(r)$. The excess free energy $f_{att}(\rho)$ corresponding to the attractive contribution is given by

$$f_{att}(\rho) = f_{LJ}(\rho) - f_{hs}(\rho), \tag{14}$$

where $f_{hs}(\rho)$ and $f_{LJ}(\rho)$ are the excess free energy for the hard-sphere contribution and for the Lennard-Jones fluid, respectively. The quasi-exact Carnahan–Starling result for the hard-sphere repulsion was used; it is given by $f_{hs}(\rho) = \eta(4 - 3\eta)/(1 - \eta)^2$, where the packing fraction η is $\eta = \pi\rho\sigma^3/6$ [16]. The empirical equation of state of Johnson *et al* [17] was used to calculate the excess free energy $f_{att}(\rho)$ for the truncated Lennard-Jones potential, where a mean-field correction is applied to the equation of state to account for the truncation and shifting of the Lennard-Jones potential:

$$f_{att}(\rho) = f_{LJ}(\rho) - f_{hs}(\rho) - \frac{\rho}{2} \int_0^{r_c} d\vec{r}\, \phi_{LJ}(r_c) - \frac{\rho}{2} \int_{r_c}^{\infty} d\vec{r}\, \phi_{LJ}(r). \tag{15}$$

The two-particle DCF $c_{att}^{(2)}(r, \rho)$ corresponding to the attractive contribution becomes

$$c_{att}^{(2)}(r, \rho) = c_{LJ}^{(2)}(r, \rho) - c_{hs}^{(2)}(r, \rho) \tag{16}$$

where $c_{hs}^{(2)}(r, \rho)$ and $c_{LJ}^{(2)}(r, \rho)$ are the two-particle DCFs for the hard-sphere contribution and for the Lennard-Jones fluids, respectively. To calculate the two-particle DCF, the integral equation with the Ornstein–Zernike integral equation was solved:

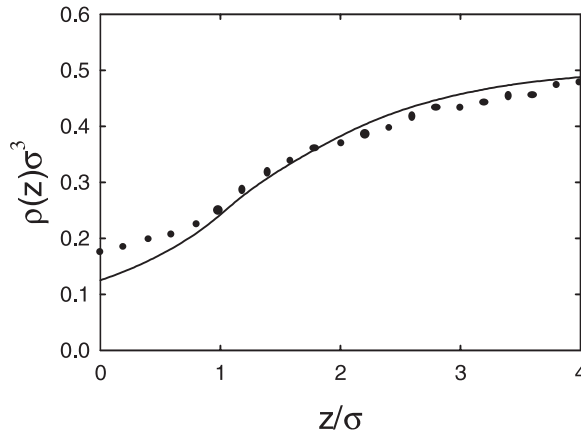$$g(r, \rho) = \exp[-\beta\phi(r) + \gamma(r, \rho) + B(r, \rho)], \tag{17}$$

Figure 1. Equilibrium particle density distributions $\rho(z)\sigma^3$ for a confined Lennard-Jones fluid at bulk density $\rho\sigma^3 = 0.5$ ($T^* = 1.35$). The solid curve and circles are from the present theory and the computer simulations [20], respectively.

where $\gamma(r, \rho) = g(r, \rho) - 1 - c^{(2)}(r, \rho)$ is the total correlation function, $g(r, \rho)$ the pair correlation function, and $B(r)$ the bridge function. For the hard-sphere system, we have used the modified Verlet bridge function $B_{\mathrm{hs}}(r, \rho)$ [18]:

$$B_{\mathrm{hs}}(r, \rho) = -\frac{1}{2}\frac{\gamma_{\mathrm{hs}}(r, \rho)^2}{1 + 0.8\gamma_{\mathrm{hs}}(r, \rho)} \tag{18}$$

where $\gamma_{\mathrm{hs}}(r, \rho) = g_{\mathrm{hs}}(r, \rho) - 1 - c_{\mathrm{hs}}^{(2)}(r, \rho)$. For the Lennard-Jones interaction $c_{\mathrm{LJ}}^{(2)}(r, \rho)$, an approximate $B_{\mathrm{LJ}}(r) = B_{\mathrm{LJ}}[s(r)]$ which was proposed by Duh and Henderson [19] is used here; it is given by

$$B_{\mathrm{LJ}}(s) = \begin{cases} -\dfrac{1}{2}\dfrac{s^2}{1 + \frac{5s+11}{7s+9}s}, & s \geqslant 0, \\ -\frac{1}{2}s^2, & s < 0, \end{cases} \tag{19}$$

with

$$s(r) = g_{\mathrm{LJ}}(r, \rho) - 1 - c_{\mathrm{LJ}}^{(2)}(r, \rho) + 4\frac{\epsilon}{k_{\mathrm{B}}T}\left(\frac{\sigma}{r}\right)^6 \exp\left[-\frac{1}{\rho\sigma^3}\left(\frac{\sigma}{r}\right)^{6\rho\sigma^3}\right]. \tag{20}$$

Throughout the numerical calculations, the diameter of a hard sphere σ was taken as the unit length. A standard Picard iteration technique was used to calculate the density distribution $\rho(z)$. To compare with the computer simulation, the Lennard-Jones potential was cut off at $r_{\mathrm{c}} = 4.0\sigma$ and shifted.

The calculated density profiles of a Lennard-Jones fluid at the reduced temperature $T^* \equiv k_{\mathrm{B}}T/\epsilon = 1.35$ are presented in figures 1–3 along with the computer simulations [20]. At bulk density $\rho\sigma^3 = 0.5$, the present theory shows a slightly lower density distribution near a hard wall compared with the computer simulations, whereas at high density it shows a slightly higher density distribution compared with the computer simulations. However, the overall picture indicates that the theoretical results are in good agreement with the computer simulations for the particle density distributions. A comparison with other approximations shows that the present theory is better than the DFPT of Tang *et al* [5, 6] based on the MCA of Barker and Henderson [7] and compares with the partitioned DFT of Zhou [21]. In the case of the DFPT based on the MCA, the critical point $T_{\mathrm{c}}^* = 1.303$ and $\rho_{\mathrm{c}}\sigma^3 = 0.275$ compares with
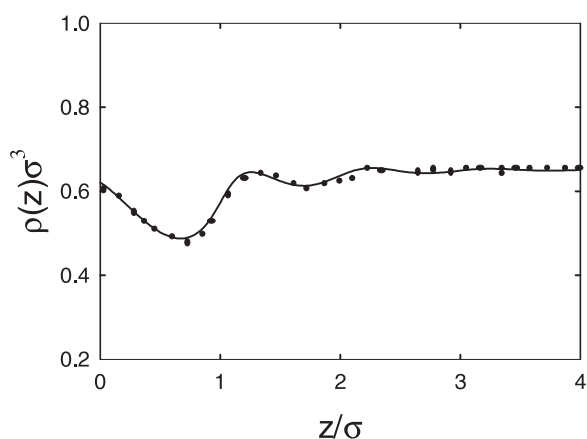
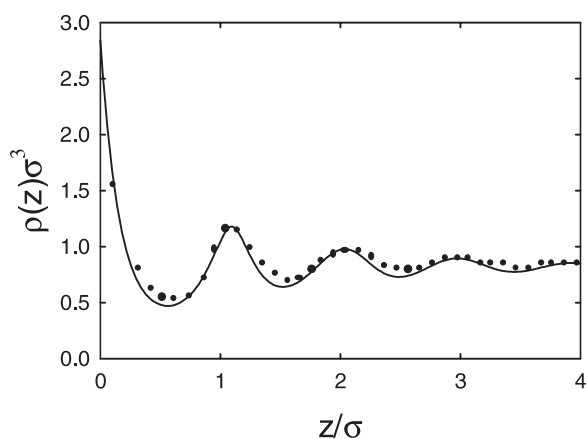**Figure 2.** As figure 1 except that $\rho\sigma^3 = 0.65$.

Figure 3. As figure 1 except that $\rho\sigma^3 = 0.82$.

the computer simulation values $T_c^* = 1.36$ and $\rho_c\sigma^3 = 0.36$ [5]. In the partitioned DFT of Zhou [21], the mixing parameter λ was specified by a hard-wall sum rule, which specifies the bulk pressure P_{bulk} via the hard-wall contact density ρ_w: $\beta P_{bulk} = \rho_w = \rho(z = 0)$. This means that for a hard planar slit, the theoretical density at the hard wall exactly coincides with that of the computer simulations. We here note that the present theory expected from figures 1–3 does not yield the correct contact density at the hard wall, because of the approximate two-particle DCF based on the bridge function [19]. However, we can obtain the correct contact density if the exact two-particle DCF and free energy are provided. On the other hand, the success of the present theory demonstrates that the WDA methods can be applied for studying the structure of the model systems with the attractive part of the potential.

3.2. Supercritical adsorption of a Lennard-Jones ethane in slit pores

As the second application, we consider the supercritical adsorption of a Lennard-Jones ethane in a graphite surface. This system has been studied previously by several authors [22–24] through computer simulations and DFPTs. In this case, the ethane is modelled by a Lennard-
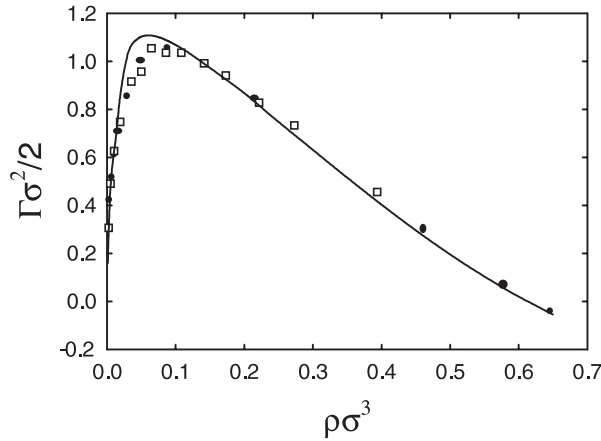
Figure 4. Adsorption isotherms of a Lennard-Jones ethene in a graphite slit ($T^* = 1.35$ and $H = 5\sigma$). The solid curve, solid circles, and open squares are from the present theory, the simulations of Sweatman [10], and the simulations of van Megan and Snook [22], respectively.

Jones potential truncated at $r_c = 2.5\sigma$ and shifted. The solid–fluid potential $u_{sf}(z)$ is modelled by a Steele 10–4–3 potential [25] with a single graphite slab:

$$u_{sf}(z) = \epsilon_w \left[\frac{2}{5} \left(\frac{\sigma_w}{z} \right)^{10} - \left(\frac{\sigma_w}{z} \right)^4 - \frac{\sigma^4}{3\Delta(z + 0.61\Delta)^3} \right], \qquad z > 0, \quad (21)$$

where z is the distance from the graphite surface, $\sigma_w = 0.903\sigma$, $\epsilon_w = 12.96\epsilon$, and $\Delta = 0.8044\sigma$. For the Lennard-Jones ethane within a graphite pore, the ethane molecule interacts with both graphite walls, so the total solid–fluid interaction, the external potential $u_{ext}(z)$, will be the sum of two terms of the type given by equation (21):

$$\beta u_{ext}(z) = \beta u_{sf}(z) + \beta u_{sf}(H - z), \tag{22}$$

where H is the width of a planar slit pore. For the graphite slit pore, the density profile expression, equation (1), becomes

$$\ln \left[\frac{\rho(z)}{\rho} \right] = -\beta u_{ext}(z) + c_{hs}^{(1)}(z; [\rho]) + c_{att}^{(1)}(z; [\rho]) - c_{hs}^{(1)}(\rho) - c_{att}^{(1)}(\rho), \qquad \text{for } 0 < z < H.$$
$$(23)$$

For the numerical calculations, the empirical equation of state of Johnson *et al* [17] was used for calculating the excess free energy $f_{att}(\rho)$ for the truncated Lennard-Jones potential, where a mean-field correction is applied to the equation of state to account for the truncation and shifting of the Lennard-Jones potential. The bridge function proposed by Duh and Henderson [19] was used to calculate the two-particle DCF $c_{LJ}^{(2)}(r, \rho)$.

The adsorption isotherms of a Lennard-Jones ethene confined in graphite slit pores with $H = 5\sigma$ and 3.5σ at the reduced temperature $T^* = 1.35$ are displayed in figures 4 and 5. Here, the adsorption isotherm Γ is defined as

$$\Gamma = \int_0^H [\rho(z) - \rho]\, dz. \tag{24}$$

As can be seen from figures 4 and 5, the theoretical calculation shows good agreement with the computer simulations [10, 22]. However, small discrepancies between the theoretical calculation and the computer simulation are found at low density. For example, the bulk density
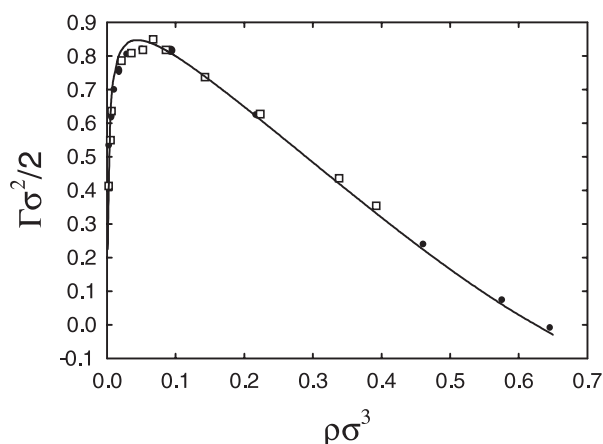
Figure 5. As figure 4 except that $H = 3.5\sigma$.

$\rho\sigma^3 = 0.093\,34$ for $H = 5\sigma$ corresponds to that at which the adsorption is a maximum [10], whereas for the present theory the maximum adsorption is found to be $\rho\sigma^3 \approx 0.058$. For $H = 3.5\sigma$, the computer simulation shows the maximum adsorption at $\rho\sigma^3 = 0.0497$, while the present theory shows the maximum adsorption at $\rho\sigma^3 \approx 0.045$. We can suggest that this discrepancy perhaps comes from the deficiencies in the description of the Lennard-Jones fluid confined in a slit pore. A comparison with other approximations [10] indicates that the present theory is better than the DFMFT (density functional mean-field theory) based both on the mean-field approach for generation of supercritical adsorption isotherms and on the effective hard-sphere diameter of Lu *et al* [26]. Actually, the adsorption isotherms predicted by the DFMFT are generally underestimated compared with the computer simulations. On the other hand, our results compare with the DFPT of Sweatman [10], although we did not display their results [10] in the figures. It is noted that the DFPT of Sweatman is based on the linear approximation for the weight density $\omega_{\text{att}}(r, \rho) = w_0(r) + \rho w_1(r)$ and the *ad hoc* assumption of the density parameter $\rho_1 = \int d\vec{r}\,|\vec{\nabla}\rho(\vec{r})|\bar{\rho}(\vec{r})/\int d\vec{r}\,|\vec{\nabla}\rho(\vec{r})|$ [10]. However, it will not be possible to obtain an accurate two-particle DCF if ρ_1 is inside the unstable spinodal region.

In figures 6 and 7, we have shown the equilibrium particle density distributions corresponding to bulk densities of $\rho\sigma^3 = 0.093\,34$ and 0.0497 with $H = 5\sigma$ and 3.5σ, respectively. For $H = 5\sigma$, the computer simulations show four pronouncedly dense absorbed layers. As expected from the adsorption isotherms predicted by the present theory, the present theory compares with the computer simulations very well. Notice here that the first high peak is strongly affected by the external potential $\beta u_{\text{ext}}(z)$. Once again, the overall picture indicates that the present theory based on the HWDA and higher-order WDA describes quite well the adsorption isotherm as well as the equilibrium particle density distribution of a Lennard-Jones ethene in a graphite slit pore. The above result along with the DFPT of Sweatman indicates that the WDA methods applied to the attractive contribution are more accurate than the DFMFT based on the mean-field approximation and the DFPT based on the MCA.

In summary, in this paper we have proposed a DFPT based on the FMT and WDAs for studying the structure of nonuniform Lennard-Jones fluids at interfaces. The theoretical results indicate that the WDA methods applied to the attractive contribution can offer a significant increase in accuracy over the DFMFT and DFPT based on the MCA. The advantages of the present theory are that: (i) it is computationally much simpler than all other DFPTs such as the first-order perturbation theory employed by Wadewitz and Winkelmann [27] and the
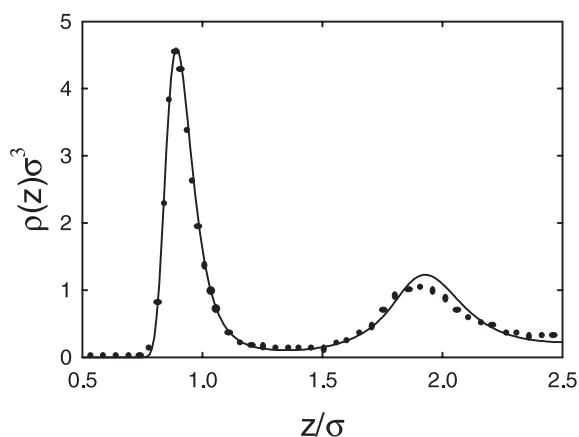
Figure 6. Equilibrium particle density distributions $\rho(z)\sigma^3$ of a Lennard-Jones ethene in a graphite slit pore at the bulk density $\rho\sigma^3 = 0.093\,34$ ($T^* = 1.35$ and $H = 5\sigma$). The solid curve and circles are from the present theory and the computer simulations [10], respectively.
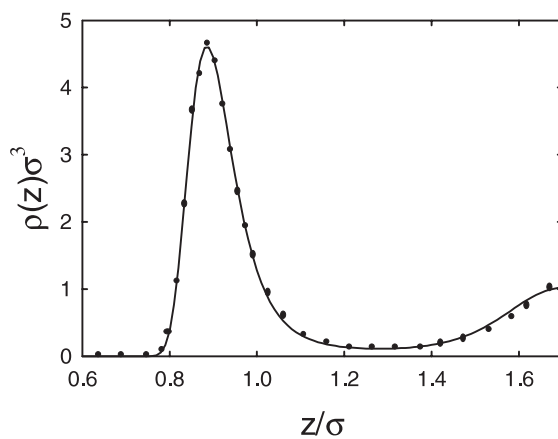

Figure 7. As figure 6 except that $\rho\sigma^3 = 0.0497$ and $H = 3.5\sigma$.

DFPT based on the MCA of Barker and Henderson [5]; and (ii) it does not require $f_{att}(\rho)$ to be consistent with the two-particle DCF $c_{att}^{(2)}(r, \rho)$ to satisfy the normalization condition $\int d\vec{r}\, w_{att}(r, \rho) = 1$, unlike other proposed WDA methods. The disadvantage is that the two-particle DCF $c_{att}^{(2)}(r, \rho)$ and the excess free energy $f_{att}(\rho)$ of model fluids come from other theories. On the other hand, it is expected that the present theory could be applicable to at least some of the model fluids confined in strong external fields, such as in capillary condensation in carbon nanopores [3, 11, 28, 29]. In this case, the phase transitions between the liquid state and the vapour state are expected from geometrical confinement. We will investigate these problems in a study in the near future.

Acknowledgments

References

[1] Evans R 1992 *Fundamentals of Inhomogeneous Fluids* ed D Henderson (New York: Dekker)
[2] Davis H T 1996 *Statistical Mechanics of Phases, Interfaces, and Thin Films* (New York: VCH)
[3] Gelb L D, Gubbins K E, Radhakrishnan R and Sliwinska-Bartowiak M 1999 *Rep. Prog. Phys.* **62** 1573
    Evans R 1990 *J. Phys.: Condens. Matter* **2** 8989
[4] Sokołowski S and Fischer J 1992 *J. Chem. Phys.* **96** 5441
[5] Tang Z, Scriven L E and Davis H T 1991 *J. Chem. Phys.* **95** 2659
[6] Varga S, Boda D, Henderson D and Sokołowski D 2000 *J. Colloid Interface Sci.* **227** 223
[7] Barker J A and Henderson D 1976 *Rev. Mod. Phys.* **48** 587
[8] van Swol F and Henderson J R 1991 *Phys. Rev.* A **43** 2932
[9] Kim S-C and Suh S-H 1997 *J. Korean Phys. Soc.* **31** 708
[10] Sweatman M B 2001 *Phys. Rev.* E **63** 031102
[11] Sweatman M B 2002 *Phys. Rev.* E **65** 011102
[12] Patra C N and Ghosh S K 2002 *Phys. Rev.* E **66** 012501
[13] Denton A R and Ashcroft N W 1989 *Phys. Rev.* A **39** 426
[14] Rosenfeld Y, Schmidt M, Löwen H and Tarazona P 1997 *Phys. Rev.* E **55** 4245
    Rosenfeld Y 1988 *Phys. Rev.* A **42** 5978
[15] Leidl R and Wagner H 1993 *J. Chem. Phys.* **98** 4142
[16] Carnahan N F and Starling K E 1969 *J. Chem. Phys.* **51** 635
[17] Johnson J K, Zollweg J A and Gubbins K E 1993 *Mol. Phys.* **78** 591
[18] Verlet L 1980 *Mol. Phys.* **41** 183
[19] Duh D and Henderson D 1996 *J. Chem. Phys.* **104** 6742
[20] Balabanić C, Borstnik B, Milêcić R and Sokolić F 1974 *Static and Dynamic Properties of Liquids* (*Springer Proceedings in Physics* vol 40) (Berlin: Springer) p 70
[21] Zhou S 2003 *Phys. Rev.* E **68** 061201
[22] van Megan W and Snook I K 1985 *Mol. Phys.* **54** 741
[23] Walton J and Quirke N 1986 *Chem. Phys. Lett.* **129** 382
[24] Tan Z and Gubbins K E 1990 *J. Phys. Chem.* **94** 6061
[25] Steele W A 1973 *Surf. Sci.* **36** 317
    Steele W A 1974 *The Interaction of Gases with Solid Surfaces* (Oxford: Pergamon)
[26] Lu B Q, Evans R and Telo da Gama M M 1985 *Mol. Phys.* **55** 1319
[27] Wadewitz T and Winkelmann J 2000 *J. Chem. Phys.* **113** 2447
[28] Neimark A V, Ravikovitch P I and Vishnyakov A 2000 *Phys. Rev.* E **62** R1493
[29] Kim S-C and Cummings P T 2001 *Mol. Phys.* **99** 1099